13th World Conference on Earthquake Engineering
Vancouver, B.C., Canada
August 1-6, 2004
Paper No. 1433

A STUDY ON PERMANENT DISPLACEMENT OF EXPRESSWAY EMBANKMENT DURING LARGE-SCALE EARTHQUAKES THROUGH DYNAMIC CENTRIFUGE MODEL TESTS

Y. KATO[1], Y. KITAMURA[2], T. HAMASAKI[3], L. LI[4], K. SAKUMA[5] and H. TANAKA[6]

SUMMARY

Newmark sliding block analysis (referred as to Newmark's method) [1] presents a useful and practical tool for evaluation of seismic slope stability hazards. The use of this analysis has been proposed as a technique for predicting the permanent displacement in expressway embankments during large-scale earthquakes. The analysis requires assumptions about shear strength characteristics of the embankment material and failure surface behavior, and the predicted permanent displacement varies strongly depending on such parameters. To clarify the effects of these parameters on the predicted permanent displacement, a series of dynamic centrifuge model tests was conducted. On the basis of the test results, the failure surface parameters were set and the earthquake-induced rotational displacement of the sliding block was calculated using the Newmark's method. The result was sufficiently close in comparison with that of the dynamic numerical analysis method to validate the applicability of the Newmark's method.

INTRODUCTION

The use of the Newmark's method as a practical procedure for predicting the earthquake-induced permanent displacement in expressway embankments during large-scale earthquakes (named as Level 2 earthquake motion in Japanese seismic design codes) is being studied by a Working Group for Seismic Design Guideline of Expressway Earth Structures organized by Japan Highway Public Corporation [2, 3, 4]. In this procedure of prediction, the sliding block is considered a potentially unstable rigid block resting

[1] Engineer, Expressway Research Institute, Japan Highway Public Corporation, Tokyo, Japan.
Email: yoshinori.katou@jhnet.go.jp
[2] Chief Engineer, Expressway Research Institute, Japan Highway Public Corporation, Tokyo, Japan.
Email: yoshinori.kitamura@jhnet.go.jp
[3] Engineer, Technical Division, Japan Highway Public Corporation, Tokyo, Japan.
Email: tomohiro.hamasaki@jhnet.go.jp
[4] Senior Researcher, Research & Development Center, Nippon Koei Co., Ltd., Ibaraki, Japan.
Email: a5109@n-koei.co.jp
[5] Chief Engineer, Tokyo Branch, Nippon Koei Co., Ltd., Tokyo, Japan. Email: a4437@n-koei.co.jp
[6] Director, Research & Development Center, Nippon Koei Co., Ltd., Ibaraki, Japan.
Email: a2738@n-koei.co.jp

on a rigid-perfectly plastic interface. It assumes that permanent displacement initiates when earthquake-induced inertial force acting on the sliding block exceed the yield resistance of the slip surface. Sliding displacement continues until the inertial forces fall below the yield resistance, and the relative velocities of the sliding block and underlying ground coincide. The permanent displacement of the sliding block may be calculated by integrating the relative velocity during slippage as a function of time. This procedure has also been used to evaluate the seismic slope stability of fill dams during earthquakes (e.g., Watanabe-Baba's method [5]).

The Newmark's method is based on the following simplifying assumptions: (a) displacements occur along a single, well defined slip surface; (b) the embankment material behaves in a rigid-perfectly plastic manner; and (c) the embankment material does not undergo strength loss under earthquake loading. It is known that the prediction accuracy of permanent displacement for road embankments during earthquakes using the Newmark's method varies significantly depending on parameters such as the shape of the defined slip surface, the applied earthquake motion and acceleration level, and shear strength characteristics of the fill material. Hence the important issues in verifying serviceability and earthquake resistance of road embankments when using the Newmark's method are how to reasonably determine the parameters and to clearly identify the items that need to pay particular attention in its application.

Under such background, a series of dynamic centrifuge model tests was conducted in which the frequency characteristics of the input motion and the construction density of the embankment were varied to simulate the seismic deformation behavior of embankments during large-scale earthquakes. This enabled confirmation of the earthquake resistance and the failure patterns of the road embankment. On the basis of the test results, the parameters for slip surface were set and the rotational displacement was calculated using the Newmark's method. The calculated rotational displacement was then compared with the result drawn from the dynamic numerical analysis to validate the applicability of the Newmark's method.

This paper presents the results of the dynamic centrifuge model tests, along with an evaluation of the earthquake resistance of the road embankments on the basis of the test results, and a discussion on the applicability of the Newmark's method as a practical procedure for predicting the permanent displacements of the road embankments during large-scale earthquakes.

SIMULATION OF THE SEISMIC DEFORMATION BEHAVIOR OF ROAD EMBANKMENT DURING EARTHQUAKES THROUGH CENTRIFUGE MODEL TEST

Dynamic centrifuge modeling system

The test program was carried out using the dynamic geotechnical centrifuge system (Figure 1) located at the Research & Development Center of Nippon Koei Co., Ltd. The centrifuge device is composed of a balanced arm with dual swing platforms and has an effective radius of 2.60 m. The design maximum centrifugal acceleration is 250 G (100 G for dynamic tests) for a normal capacity of 981 G-kN. The centrifuge is equipped with a data acquisition system with 30 digital dynamic amplifier channels, of which 18 channels are voltage charge amplifiers. The data acquisition system is coupled with a data processing system that enables on-line monitoring of the measured data. Electric signal transmission is via fiber-optical slip-rings to provide the acquisition of noise-free precise data. The centrifuge is equipped with rotary joints for the transmission of electric power and hydraulic pressure to the centrifuge mounted shaker and test model.

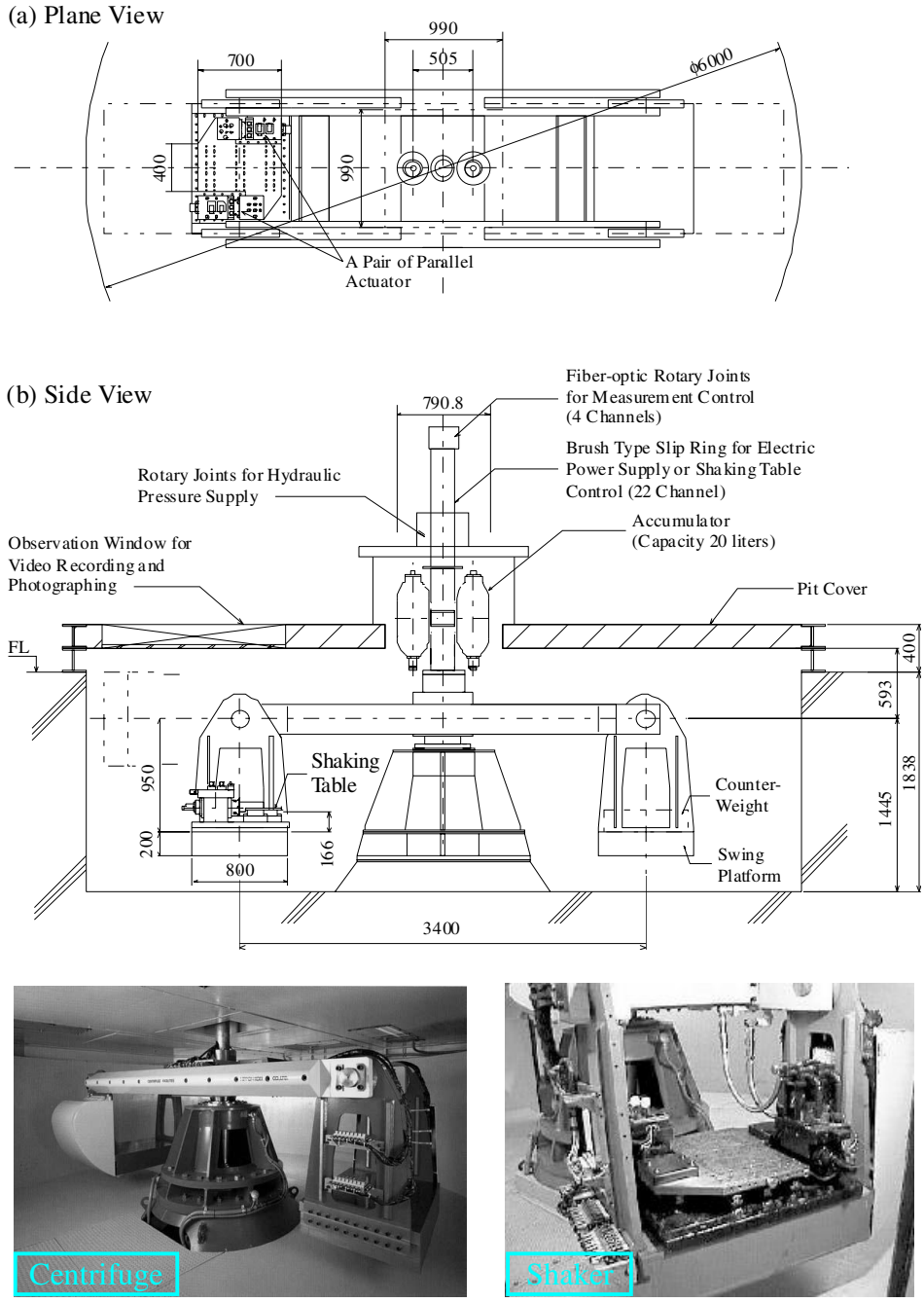

Figure 1 Configuration of the dynamic centrifuge system

The shaker is equipped with a rectangular slip table and is driven by a pair of actuators controlled by an electro-hydraulic servomechanism. By using an automatic feedback control system the shaker can produce both regular and irregular target motions in the model with high precision. A technical report given by Tanaka and Li [6] can be referred to the detail specification of the dynamic centrifuge system.

Model, test conditions and procedures

A 1/50 scaled model with 2-D plane strain condition was used in the test program to simulate the prototype slope of the expressway embankment with a height of 20 m and a standard slope gradient of

1:1.8. Considering the size of the model container, a half section model with a crest width of 15 m in prototype scale was adopted. Figure 2 shows the schematic layout of the test model and its instrumentations. The material used for the embankment models was a sandy soil and two types of model compaction densities Dc=90% and 100% were set according to the quality control guideline for the construction of expressway embankments. The surface grounds for characterizing the input motion (i.e., base grounds of the embankment) were assumed to be type I or type III based on the Japanese seismic design code. Of the type II surface wave motion specified in the "Specifications for Highway Bridges Part V: Seismic Design" (Japanese Road Association [7]), the NS component of the wave motion recorded at the Kobe Meteorological Observatory (JKN) and the NS component of the wave motion recorded at Kobe Port Island (PIN) were used as input motions for type I and type III surface grounds, respectively. The maximum acceleration amplitude was adjusted to 460 gal to match the capacity of the shaker. The test program was conducted on three models (referred to as CASE1 to CASE3) with combinations of different compaction densities and input motion as parameters. Table 1 shows the test conditions. Two types of input motions with their frequency characteristics are shown in Figure 3.

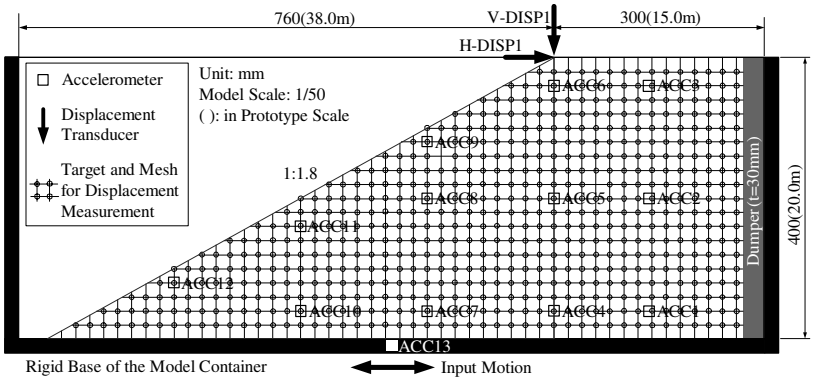

Figure 2 Schematic layout of the test model and its instrumentations

Table 1 Test conditions

Test Case	Input Motion	Compaction Density
CASE1	JKN Wave for Type I Base Ground	Dc=90%
CASE2	PIN Wave for Type III Base Ground	Dc=90%
CASE3	JKN Wave for Type I Base Ground	Dc=100%

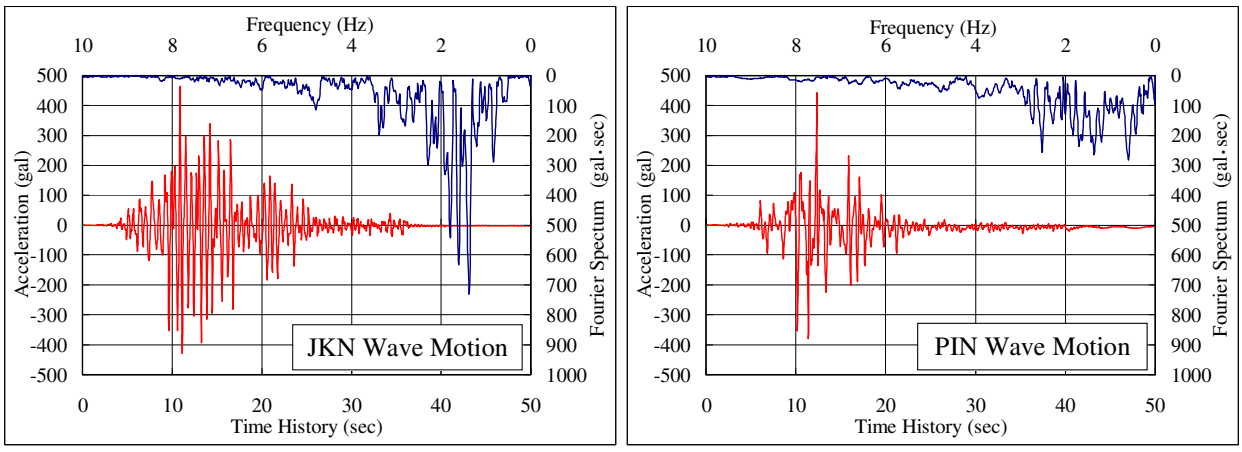

Figure 3 Input motion and frequency characteristics

The model embankment was prepared using a rigid model container made of aluminum alloy (glass plated on the front for the visualization of the model behavior during test) with internal dimensions of 1060 mm in width, 400 mm in height and 295 mm in depth, by compacting model material with a density controlled so as to form soil layers vertically with a thickness of 4 cm per layer. Considering reproducibility of the material properties, the material used for the model embankment was a mixture by blending Toyoura silica sand and Kaolin clay in a dry weight ratio of 9:1, and then adding water to the optimum moisture content. Table 2 shows the physical and mechanical properties of the model material. Figure 4 shows the stress-strain relationships together with the volume change of the model material at a degree of compaction Dc=90% obtained from a tri-axial compression test with drain condition. On the basis of this information, it is clear that the model embankment material shows no clear peak strength for any confining pressure and has negative dilatancy characteristics, so that the progress of shear deformation will be accompanied by volumetric shrinkage.

Table 2 Properties of the model embankment material

Soil Particle Density ρ_s		g/cm^3	2.647
Soil Particle Distribution and Maximum Particle Diameter	Sand	%	90
	Silt	%	4
	Clay	%	6
	d_{max}	mm	0.425
Compaction Properties	ρ_{dmax}	g/cm^3	1.73
	w_{opt}	%	11.8
Strength and Dynamic Deformation Properties of the embankment material at Dc=90%	ρ_t	g/cm^3	1.741
	c_d	kN/m^2	1.39
	ϕ_d	°	33.8
	Shear Modulus	$G_0=16695+327.63\sigma_c'$	(kN/m^2)
	Dumping	$h=31.75+0.0202\sigma_c'$	(%)
Strength and Dynamic Deformation Properties of the embankment material at Dc=100%	ρ_t	g/cm^3	1.934
	c_d	kN/m^2	16.91
	ϕ_d	°	38.9
	Shear Modulus	$G_0=20035+428.97\sigma_c'$	(kN/m^2)
	Dumping	$h=33.4+0.0001\sigma_c'$	(%)

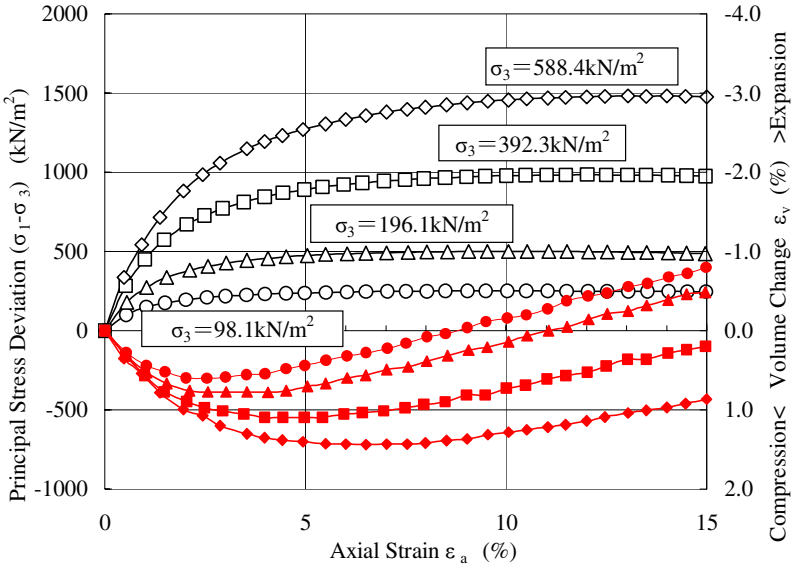

Figure 4 Stress-strain relationship for the model embankment material at Dc=90%

Silicon rubber cushioning material with a thickness of 30 mm was inserted at the boundary surfaces between the embankment model and the side wall of the model container as a dumper to eliminate the influence of wave transmission from the rigid container wall. 180# sandpaper (JIS R 6010) was affixed to the bottom of the model container to produce a rough boundary condition. As the test procedures, the model was subjected to a centrifugal acceleration field of 50 G (G: gravitational acceleration) first to reach a stable self-weight loading state, then specified input motion as shown in Figure 3 was applied to the model at the same acceleration level for 5 times excitation in a step-by-step manner. Among the strong excitation, a low level excitation with white noise wave was also applied to the model to verify the change of acceleration response of the model embankment due to the permanent deformation.

Measurements were taken of the response acceleration in the embankment and the displacement at the shoulder of the slope. Displacement measurements by means of the reference mesh and targets were taken in gravitational field (1G) by stopping the centrifuge after the first and fifth excitation.

Test Results and Observations

Permanent deformation patterns in embankments during an earthquake

Figure 5 shows the permanent deformation of the embankment followed the first excitation using JKN wave with the maximum input acceleration amplitude of 460 gal for CASE1. Figures (a) to (c) show the permanent displacement vectors, calculated permanent shear and volumetric strain distributions respectively. The figure confirms the following with regard to the permanent deformation patterns in embankments during an earthquake:

(1) Limited to the test conditions used here, the permanent deformation in an embankment resulting from the excitation is concentrated in the surface layers from the middle location of the slope up to the area around the shoulder. The permanent displacement vectors are largest close to the shoulder and angle downwards more sharply than the gradient of the slope itself. However, the vector decreases toward the tail of the slope and the direction matches almost the slope gradient.

(2) Although clear failure surface in the slope could not be confirmed, the area of permanent shear strain concentration is clearly sensible, and the pattern of permanent deformation is primarily sliding deformation accompanying shear. The area with the greatest concentration of the shear strain is at a depth of 3 to 4 meters in prototype below the slope surface, and the behavior of the surface layer from the middle location of the slope to the shoulder was similar to that of a solid sliding block.

(3) In terms of volumetric deformation caused by the excitation, volumetric compression deformation accompanying shear deformation is the most frequent, while the distribution of volumetric compression strain almost exactly duplicates the shear strain distribution, showing a deformation pattern that conforms to the dilatancy characteristics of the embankment material (see Figure 4). The area close to the crest of the embankment shows the effects of tensile deformation in the form of volumetric strain on the expansion side, and the volumetric strain inside the embankment is smaller than that in the surface layer.

In summary, under the conditions used in this test program, horizontal displacement due to shear deformation occurred in the area close to the surface of the slope where shear strain was concentrated. At the same time, volumetric compression occurred due to negative dilatancy, and consequently resulting in the behavior conducive to the decrease of horizontal displacement in the middle location of the slope surface. This indicates that the permanent deformation pattern for embankments in an earthquake is strongly governed by the dynamic shear deformation and its accompanying volumetric deformation. In the other words, this suggests that differences in the properties of the fill material used in the embankment have a major impact on the permanent deformation pattern during an earthquake.

Figure 6 shows deformation in the embankment slope after 5th excitation at the same input acceleration level for CASE1. This shows that there is no large-scale collapse sufficient to be recognized as a sliding block and that the deformation behavior of the embankment during an earthquake demonstrates strong and tenacious performance.

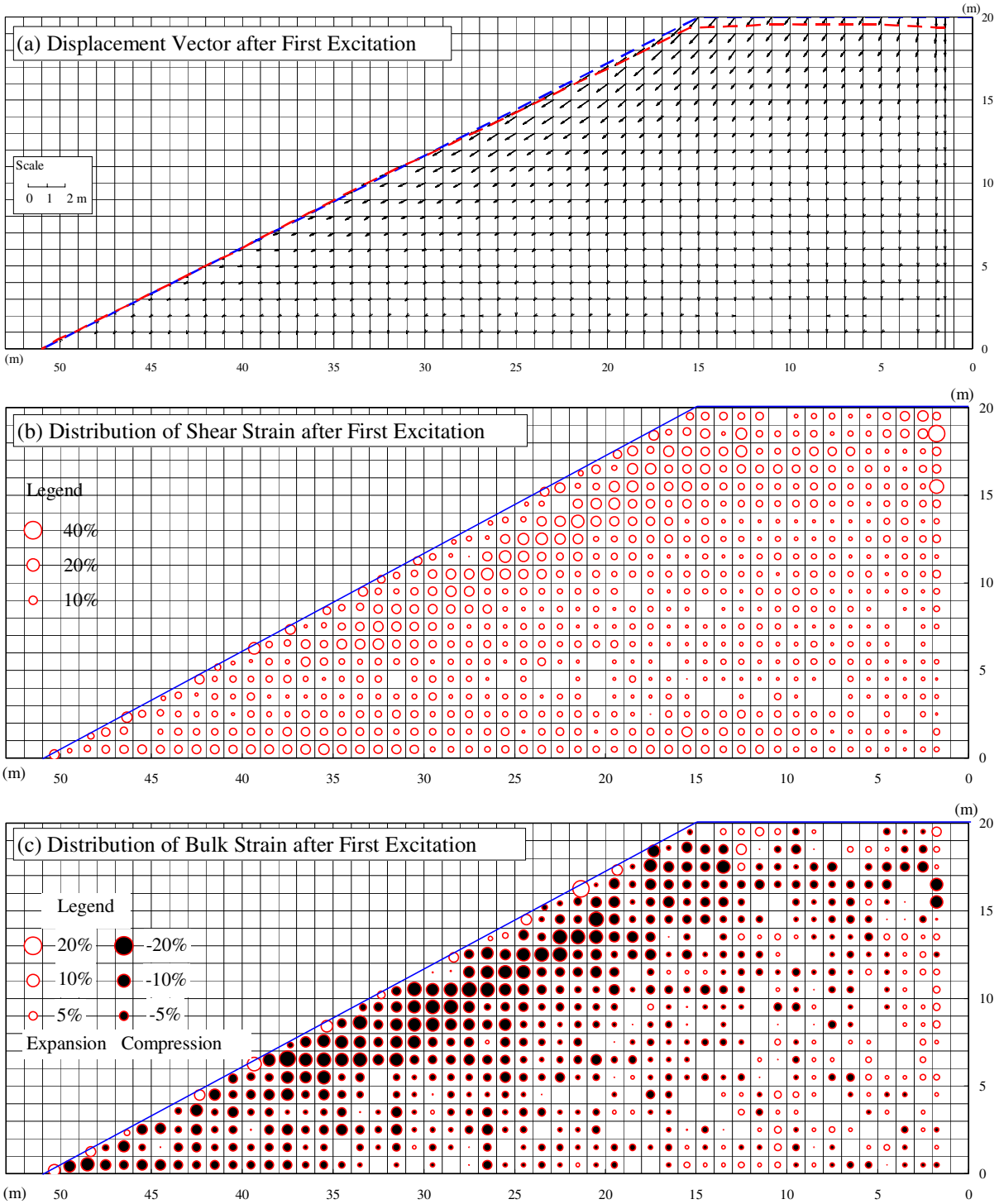

Figure 5 Permanent deformation of the embankment after the first excitation for CASE1 (in prototype scale)

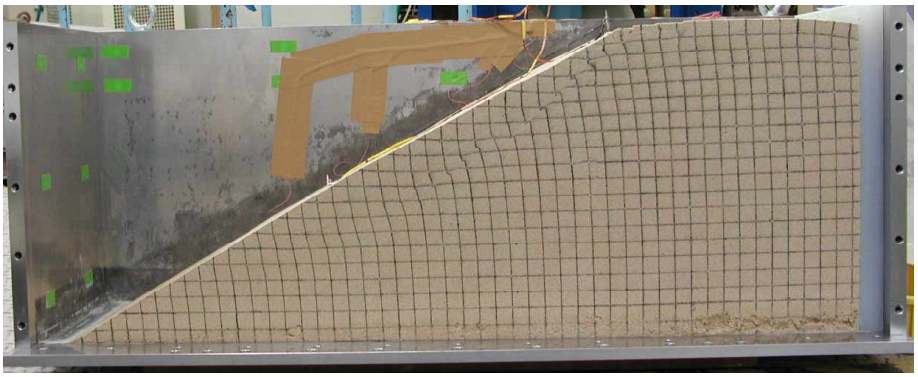

Figure 6 Deformation of the embankment after 5th excitation for CASE1

Differences in deformation of the embankments due to input motion and compaction density

Figure 7 shows the changes of the accumulated settlement and horizontal displacement in prototype scale at the shoulder of the embankment slope versus the number of applied strong excitation for the three test cases. This confirms the following items regarding the effects of changes to the input motion and compaction density on the permanent displacement at the shoulder of the embankment slope during earthquakes.

(1) Regardless of test parameters such as the input motion and compaction density, the accumulated settlement and horizontal displacement at the shoulder of the embankment slope showed similar trends limited to the present test conditions such as the cross-sectional shape of the embankment and materials.

(2) For the same compaction density (Dc=90%) and peak input acceleration level, the displacements at the shoulder of the embankment slope for Type I surface ground input motion (CASE1: JKN, dominant frequency f=1.4 Hz) are nearly twice larger than that for Type III surface ground input motion (CASE2: PIN, dominant frequency f=0.6 Hz). Such differences in the displacement are considered to be caused by the differences between the natural frequencies of the embankments and the frequency characteristics of the input motion and the number of repetitions of the principal seismic motion (see Figure 3).

(3) For the same embankment material, the permanent displacement at the shoulder for Dc=100% is approximately 1/5 of that for Dc=90%, showing that improving the construction control standards can greatly reduce the earthquake-induced permanent deformation of embankment slopes.

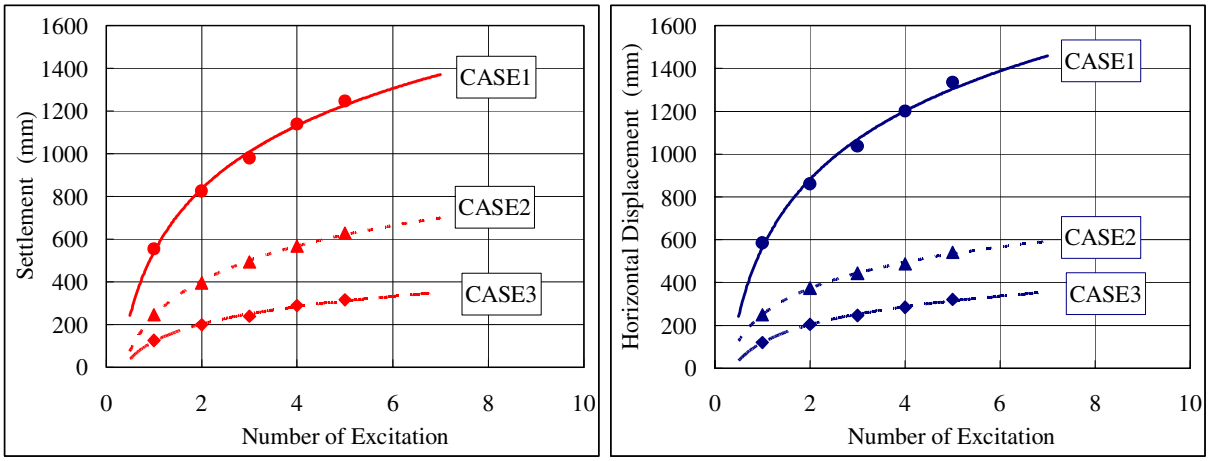

Figure 7 Accumulated settlement and horizontal displacement during excitation (in prototype scale)

Acceleration response characteristics inside the embankment

Figure 8 shows the distributions of the acceleration response rates along the vertical lines inside the embankment close to shoulder of the slope (A-A' and B-B') for the three test cases. These data were measured from the excitations by using low level white noise waves with peak acceleration amplitude less than 50 gal applied after first, third and fifth strong excitations. From these charts, it can be seen that for lines A-A' (ACC4 to 6) and B-B' (ACC7 to 9), the acceleration response rate inside the embankment relative to the input acceleration shows a tendency to increase towards the surface of the embankment, with amplitudes of approximately 3 to 4 times. In the process of excitation, this tendency in the acceleration response rate remains almost no changes in CASE2 and CASE3 where the embankment deformation is slight. However, in CASE1 where relatively large deformation occurred, as the number of applied excitation increases there is an observable tendency towards striking reductions in the acceleration response rate in the vicinity of the embankment surface, bounded by the area in which the shear strain is concentrated (see Figure 5). Such changes of the acceleration response rates could be considered to be caused by the weakening of the rigidity in locations where deformation is concentrated due to accumulated shear strain during earthquakes, and consequentially decline in response above these locations. On the other hand, the acceleration response rates after third excitation in the lower part of the embankment show a tendency to increase slightly when compared with that before strong excitation in CASE1. This may probably be considered to be caused by the increase of the rigidity due to densification of the embankment at the lower part accompanying with the excitation-induced compaction.

DISCUSSION ON THE APPLICABILITY OF THE NEWMARK SLIDING BLOCK ANALYSIS FOR PREDICTING THE EARTHQUAKE-INDUCED PERMANENT DISPLACEMENT

On the basis of the results drawn from the centrifuge model tests, the permanent displacement of the sliding block was estimated. Through comparing the test results with those acquired using the Newmark sliding block analysis, the applicability of the Newmark sliding block analysis as a practical tool for predicting the earthquake-induced permanent sliding displacements in embankment slopes was evaluated.

Measured permanent displacement for comparing with that predicted by using the Newmark sliding block analysis

Settlement caused by the motion of sliding block

The earthquake-induced permanent deformation in the embankment slope measured from the centrifuge model test was confirmed as the combination of the compacting settlement at the whole thickness of the embankment (δ') and the sliding settlement caused by the motion of the sliding block (δ). For test CASE1 in which large permanent deformation occurred during excitation, displacements at the crest of the embankment after the first excitation are as shown in Figure 9(1), the sliding settlement caused by the motion of the sliding block at a distance of 3.3 meters from the shoulder is measured as δ=8.3 cm in prototype scale. Figure 9(2) shows the vertical displacements at the points on the crest of the embankment after the first excitation. The compacting settlement (δ') is roughly measured as 45 cm in prototype scale. Of these two settlement components, the permanent displacement that can be evaluated using the Newmark's method is the sliding settlement caused by the motion of the sliding block (δ).

Slip surface

Since the shape and position of the slip surface was hard to visually determine from the test result, the mesh elements with large shear strain (γ>10%) were picked up from the shear strain distribution chart for fitting the slip surface (solid line), where the shape of the slip surface was assumed to be an arc. Figure 10 shows the fitted slip surface. As a reference, the slip surface with the minimum yield acceleration calculated on the basis of the limit equilibrium method was also plotted in the figure as dotted line.

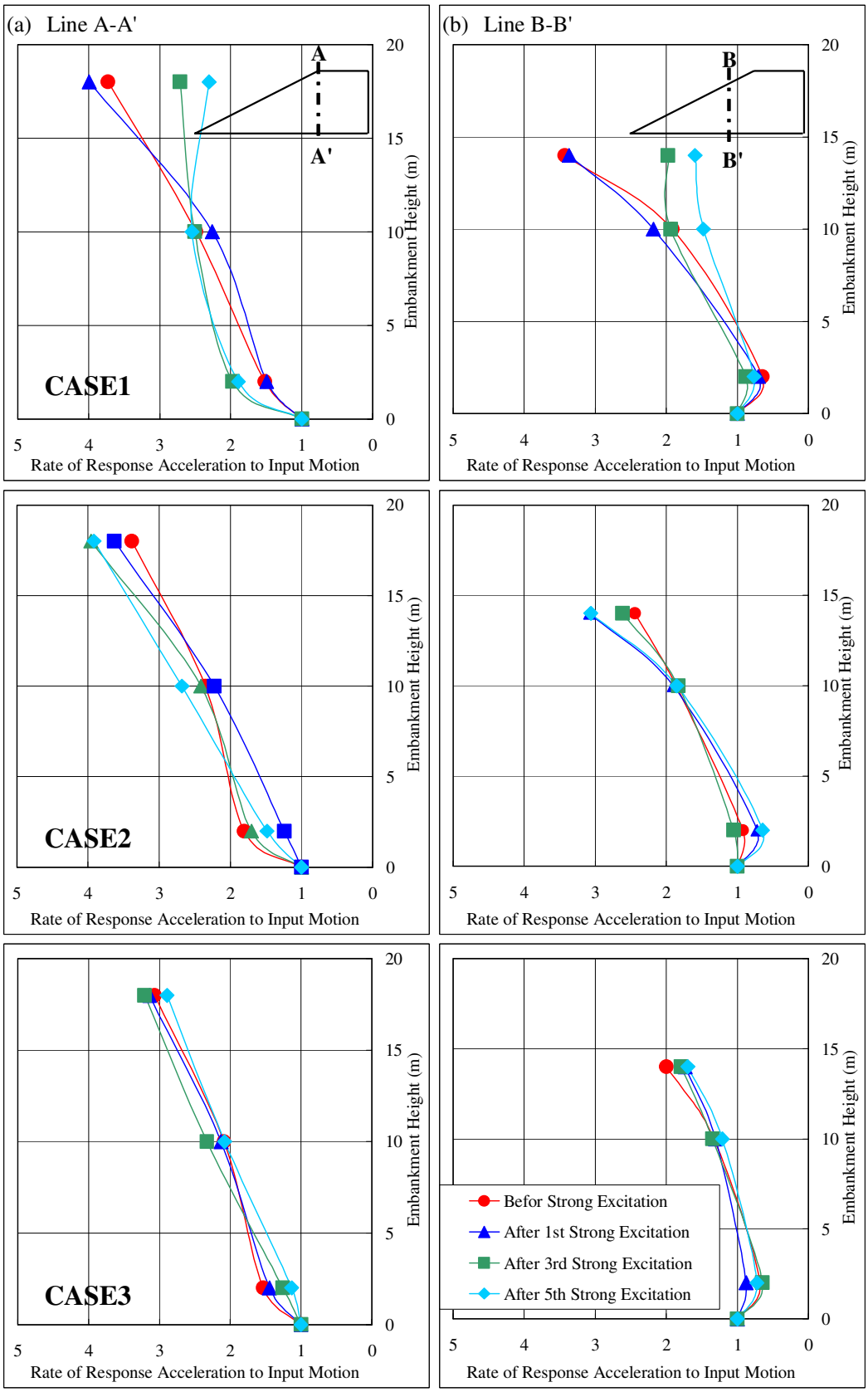

Figure 8 Rate of response acceleration in the embankment relative to the input motion

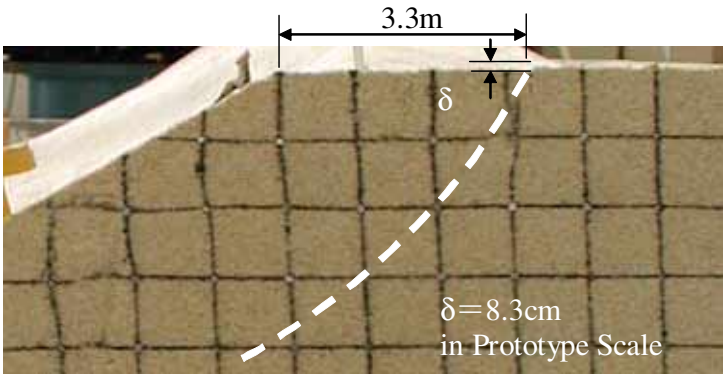

(a) Settlement of the embankment shoulder due to sliding

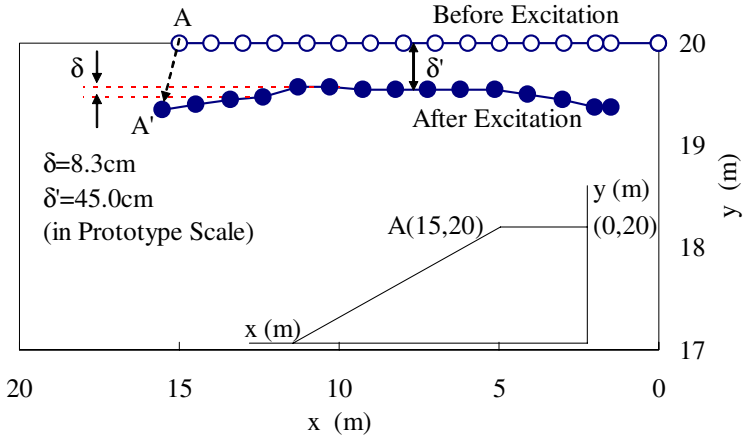

(b) Deformation of the embankment crest after excitation

Figure 9 Permanent displacement of the embankment crest after excitation (in prototype scale)

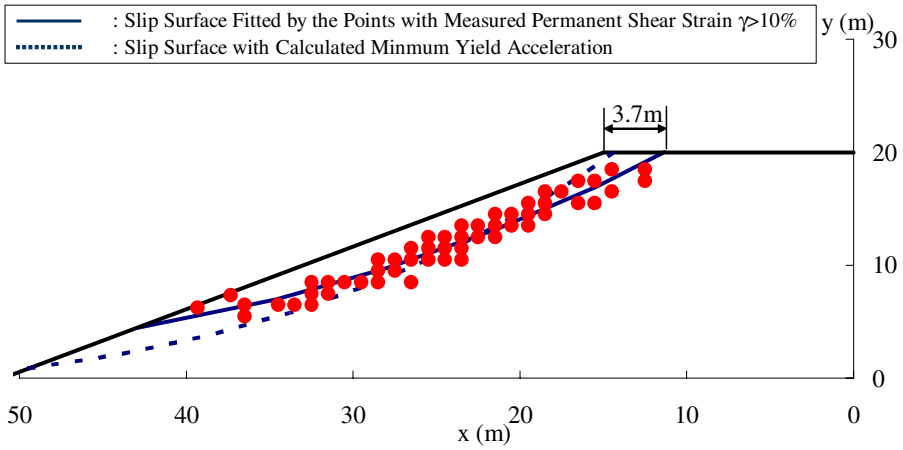

Figure 10 Slip surface set based on test result for the Newmark sliding block analysis

Slip surface rotational displacement predicted by using the Newmark sliding block analysis

The rotational displacement was calculated using the Newmark's method for the slip surface fitted from the distribution of the shear strain measured for CASE1 as shown in Figure 10. The analysis parameters and input motion are as shown in Table 2 and Figure 3 respectively. Because the embankment material

used in the test showed negative dilatancy and almost no difference between its peak and residual strength, constant strength parameters obtained from the peak strength as shown in Table 2 were adopted for the calculation of the excitation-induced rotational displacement.

Figure 11 shows the rotational displacement calculated by using an algorithm [8] based on the Newmark's method. An additional line has been added to the figure indicating the time where the incremental rotational displacement reaches at its peak value (5.43 to 5.77 sec). The yield acceleration for the measured slip surface was 196 gal and a total rotational displacement of 6.2 cm was obtained.

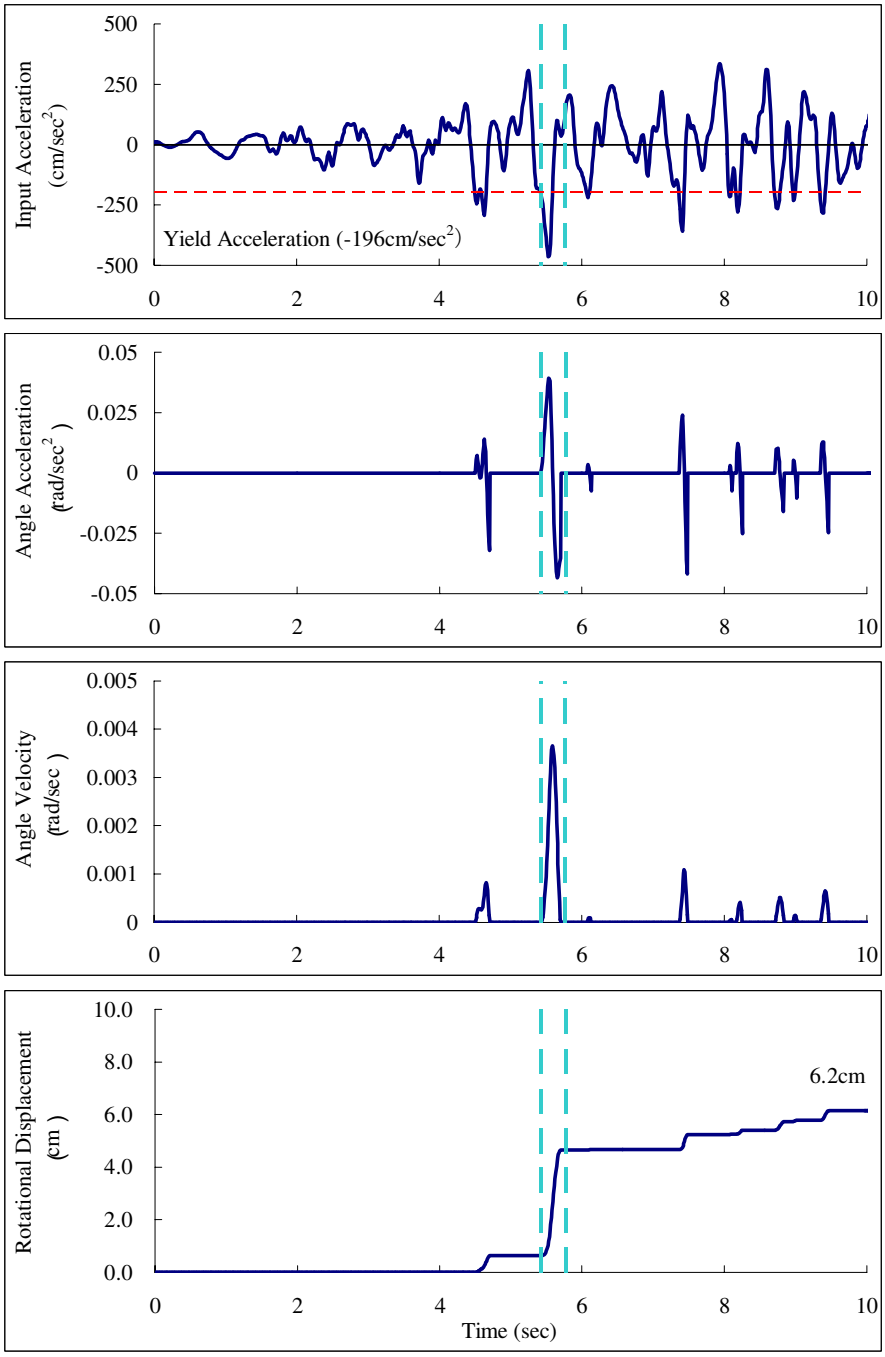

Figure 11 Rotational displacement calculated by using the Newmark sliding block analysis

Discussion on applicability of the Newmark sliding block analysis for predicting earthquake-induced permanent displacement in the embankment

Figure 12 shows the sliding settlement (in strictly accurate terms the maximum variation in levels at the crest) in the crest of the embankment measured after the first excitation for CASE1, along with the rotational displacement of the sliding block calculated using the Newmark's method. The value of sliding displacement (converted to rotational displacement as the Newmark's method) calculated using the Watanabe-Baba's method, which is widely used in prediction of earthquake resistance in fill dams is also shown in the figure. While the Watanabe-Baba's method is based on the same concepts as the Newmark sliding block analysis, it takes into account the amplitude of the acceleration response in the embankment in terms of dynamic numerical analysis as well as the effects of the vertical earthquake motion, while also estimating the changes in the yield acceleration in the slip surface progressively against a time log in its calculations of the sliding displacement. Although the definition of the sliding settlement obtained from the test result as shown in this figure is different from those of the rotational displacements predicted using the Watanabe-Baba's method and the Newmark's method in strictly accurate terms, based on considerations such as the effects of the analytical precision etc., they were compared on the basis that the rotational displacement is approximately equal to the sliding settlement. From these investigations, the following findings were drawn regarding the applicability of the Newmark's method as a practical procedure for predicting the permanent deformation in road embankments during large-scale earthquakes.

(1) With regard to the slip surface settings for the Newmark's method, an arc fitted with the measured shear strain distribution was adopted. The rotational displacement calculated with this slip surface was roughly coincident with the sliding settlement measured from the test. As shown in Figure 10, however, the slip surface with calculated minimum yield acceleration is quite different from the fitted arc, and a rotational displacement of 37 cm was predicted for the calculated slip surface. Thus, the parameter setting for the slip surface in prediction of the earthquake-induced permanent displacement has a major effect on the predicted results. In order to improve the prediction accuracy, a practical and effective method should first be developed for setting reasonable slip surface parameters when the Newmark's method was used as the procedure for predicting the earthquake-induced earthquake.

(2) The rotational displacement for sliding block predicted using the Newmark's method can explain the sliding settlement measured from the test with the accuracy requirement for practical utilities. Accordingly, as a practical tool for the earthquake resistance of embankments, the Newmark's method can effectively be applied for the prediction of rotational deformation of the sliding block. More case studies for different conditions are necessary to validate the prediction accuracy.

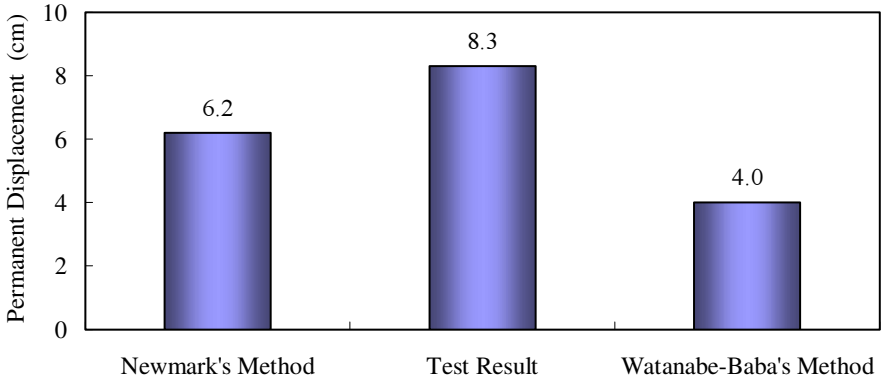

Figure 12 Comparison of the permanent displacements between test and analyses

(3) By comparing the prediction value drawn from the Newmark's method with that from the Watanabe-Baba method in which the dynamic analysis is needed, there was an error less than 2 cm for an embankment with a height of 20 m, it is considered that the Newmark's method can serve as a practical procedure for predicting the earthquake-induced permanent displacement in road embankments.

CONCLUSIONS

With the aim of verifying the applicability of the Newmark's method as a practical procedure for predicting the earthquake-induced permanent displacement in road embankments, a series of dynamic centrifuge model tests was performed in which the frequency characteristics of the input motions and the compaction density of the embankment were varied. The seismic deformation behavior of the embankment during an earthquake was ascertained. On the basis of the test results, the measured sliding settlement was compared with that predicted by using the Newmark's method, and the applicability of the Newmark's method was then evaluated. The main findings and conclusions are as follows:

(1) The deformation pattern for an embankment during an earthquake is greatly influenced by the characteristics of the embankment materials. It is affected particularly strongly by the shear characteristics and their accompanying dilatancy characteristics. The confirmation of these dependent relationships and their application as the procedure for evaluating earthquake resistance are the important subjects in the further study of earthquake resistance of the road embankment.

(2) In terms of the behavior of embankments during an earthquake, strictly quality controlled embankments show considerably strong to earthquake and do not easily collapse even deformation occurs to a certain extent during large-scale earthquakes.

(3) The permanent deformation in an embankment is strongly dependent on parameters such as the frequency characteristics of the input motion, the number of principal seismic motion repeated, and the initial shear modulus of the embankment.

(4) Shear deformation in the embankment caused by earthquake history has an impact on the rigidity of the embankment, and this, coupled with variations in the acceleration response characteristics of the embankment, then affects the deformation behavior of the embankment again. These dependency relationships lead to large variations in the earthquake-induced permanent deformation of the embankments.

(5) With regard to the applicability of the Newmark's method, it was confirmed that as a practical procedure the Newmark's method is effective for predicting the earthquake resistance of the embankments, and it was also reconfirmed that accurate prediction of the earthquake-induced permanent displacement needs to develop a practical and effective method for setting the parameters for the slip surface.

REFERENCES

1. Newmark N. M. "Effects of earthquake on dams and embankments." Geotechnique, 15(2), 1965: 139-160.
2. Kato Y., Ogata K., Li L., Tanaka H., Shimomura S. and Sakuma K. "A study on permanent displacement under large-scale earthquake – (part 1) Dynamic centrifuge model test." Proceedings of the 38th JGS annual meeting, 2003: 1309-1310.
3. Kato Y., Kitamura Y. Hamasaki T. Sakuma K. Li L. and Sugiyama H. "A study on permanent displacement under large-scale earthquake – (part 2) Discussion on the estimation methods for

permanent displacement of road embankment." Proceedings of the 38th JGS annual meeting, 2003: 1307-1308.
4. Kato Y., Kitamura Y., Li L. and Tanaka H. "Discussion on the permanent displacement of expressway under large-scale earthquake." Proceedings of the 58th JSCE annual meeting, 2003: 435-436.
5. Watanabe H. and Baba K. "Discussion on the evaluation procedure for slope stability of fill dam based on seismic analysis." Japan Commission on Large Dams: Large dams, No. 97, 1981: 25-38
6. Tanaka H. and Li L. "Dynamic centrifuge model test on seismic performance of the changing points of underground structures." Civil Engineering Journal, Japan: Public Works Research Center, Vol. 45, No.1, Jan. 2003: 46-49.
7. Japanese Road Association "Specifications for highway bridges, Part V: Seismic design." 2002.
8. Tateyama M., Tatsuoka F., Koseki J. amd Katsumi H. "Studies on seismic design method of soil structures." RTRI report, Japan, Vol. 12, No. 4, April 1998: 7-12.